

Supporting Information

Assembling and ordering polymer-grafted nanoparticles in three dimensions

Honghu Zhang, Wenjie Wang, Mufit Akinc, Surya Mallapragada, Alex Travasset, and David Vaknin
Ames Laboratory, Iowa State University, Ames, Iowa 50011, USA

Form Factor of AuNPs

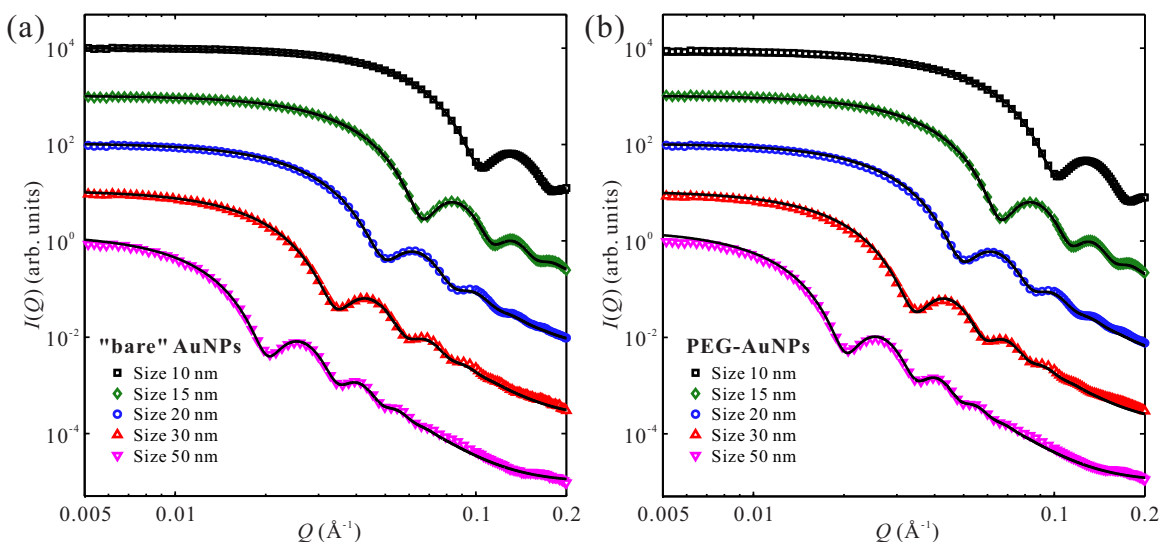


Fig. S1 SAXS profiles of (a) bare (unfunctionalized) AuNPs stabilized with citrate and (b) PEG-AuNPs with various nominal core sizes. Solid lines are best fits using the form factor of spherical solid particles with polydispersity modeled by a Gaussian distribution. Plots are vertically shifted.

The form factor of AuNPs with and without PEG coating is measured by SAXS. Fig. S1 shows SAXS profiles of unfunctionalized (bare) AuNPs stabilized with citrate and PEG-AuNPs (with nominal sizes in the range of 10–50 nm as indicated) dispersed in water after background subtraction. Such SAXS data and analysis allow determination of the actual size of the particles as the nominal size provided by the manufacturer is only approximate.²¹ Here we assume that the size polydispersity obeys a Gaussian distribution function. The profile fitting of the measured form factor (solid lines in Fig. S1) provides the actual particle size and size distribution in Table S1. The actual size is slightly smaller than the nominal size, and the polydispersity (spread) is about 10 % of the mean size. We find that the measured SAXS pattern for bare AuNPs and capped PEG-AuNP are practically the same indicating that the scattering is dominated by the highly electron rich AuNPs where the PEG shell has electron density that is very close to that of the medium (i.e., aqueous solution). We therefore notice in Table S1 that particle size varies little between that of a bare AuNPs stabilized with citrate and that of PEG-AuNPs.

Table S1 Nanoparticle size distribution determined by profile-fitting of SAXS data collected from the suspension

Nominal size (nm)	Size of bare AuNPs (nm)	Size of PEG-AuNPs (nm)
10	8.5 ± 0.8	8.7 ± 0.8
15	13.3 ± 1.2	13.3 ± 1.2
20	17.6 ± 2.0	17.7 ± 1.9
30	25.5 ± 2.7	25.6 ± 2.5
50	43.4 ± 4.1	43.5 ± 4.0

Hydrodynamic size of AuNPs

The hydrodynamic size D_h of unfunctionalized (bare) AuNPs stabilized with citrate and PEG-AuNPs in aqueous solution was measured by dynamic light scattering (DLS). Fig. S2 and Table S2 show hydrodynamic size distribution of citrate-stabilized AuNPs and PEG-AuNPs (with nominal core sizes 10–50 nm). The size distribution shifts to the large size due to PEG coating.

According to our previous model⁴², the hydrodynamic size D_h of a given PEG-AuNP with Au core size D is given by

$$\left(\frac{D_h}{D}\right)^2 = 1 + 4 \frac{Nb^2\sigma^{1/2}}{D} (2w_0)^{1/4}, \quad (\text{S1})$$

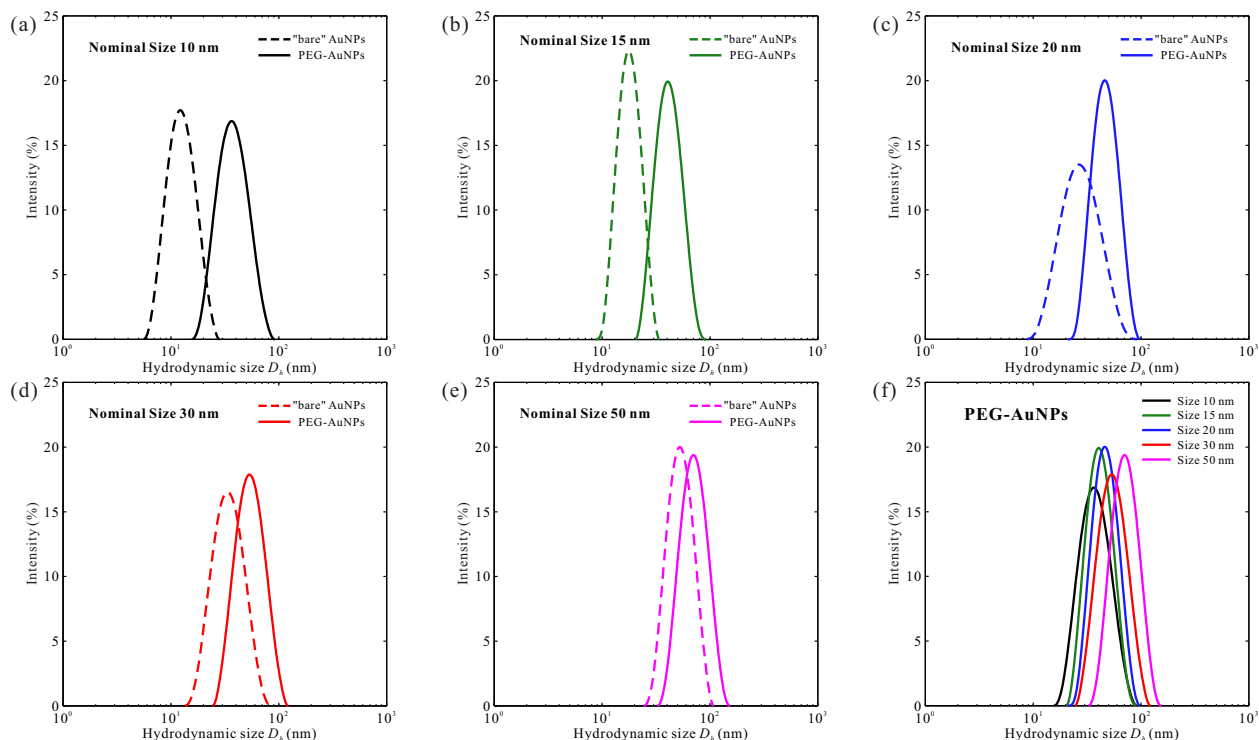


Fig. S2 Hydrodynamic sizes D_h measured by dynamic light scattering for unfunctionalized (bare) citrate-stabilized AuNPs and PEG-AuNPs with different nominal core sizes: (a) 10 nm, (b) 15 nm, (c) 20 nm, (d) 30 nm, (e) 50 nm. (f) Comparison of D_h for PEG-AuNPs with various nominal sizes.

Table S2 Hydrodynamic size distribution by dynamic light scattering before and after PEG coating. PEG coating leads to a shift of size distribution.

Nominal size (nm)	Citrate-stabilized AuNPs (nm)	PEG-AuNPs (nm)	Shift of distribution center (nm)
10	13.0 ± 3.9	39.1 ± 12.6	26.1
15	18.4 ± 4.4	42.5 ± 11.5	24.1
20	29.2 ± 11.9	49.7 ± 13.1	20.5
30	35.7 ± 11.5	56.1 ± 16.9	20.4
50	54.7 ± 14.5	73.9 ± 20.3	19.2

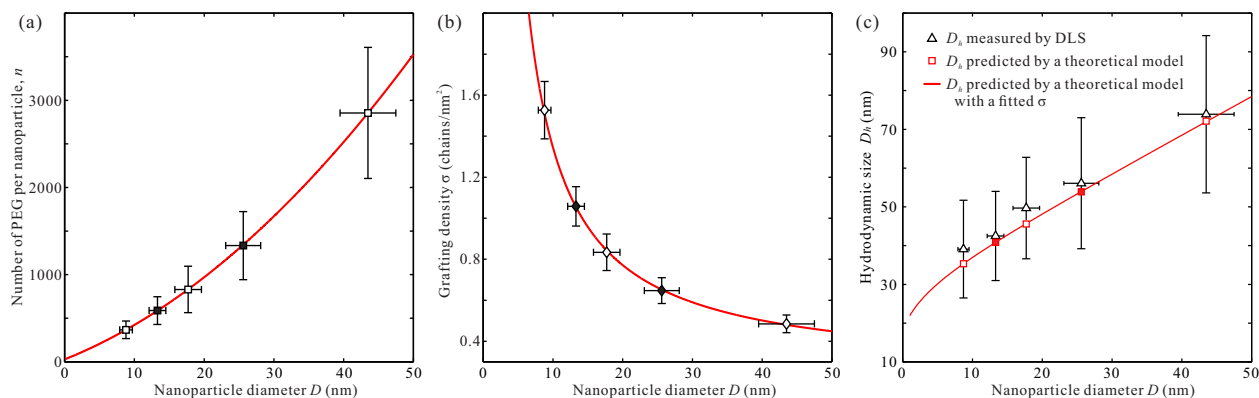


Fig. S3 (a) The number of PEG per AuNP n for various nanoparticle sizes measured by thermogravimetric analysis (TGA). The red solid line is a best fit with a polynomial function. (b) The corresponding grafting density σ . The solid line is adopted from the best fit in (a). (c) The hydrodynamic size D_h measured by dynamic light scattering (DLS) and predicted by the theoretical model of Equation S1. The solid line is calculated using the fitted σ in (b). Note that the open symbols represent the experimentally measured results while solid symbols stand for the estimated values. The error bars for D and D_h are the spread in size distribution.

where $b = 7.24 \text{ \AA}$ is the Kuhn length of PEG, $N = 68.5$ is the number of Kuhn monomers for PEG with the molecular weight of 6000, σ is the grafting density, and w_0 is a dimensionless three body interaction, where we use the Flory result $w_0 = 1/6$, so that $(2w_0)^{1/4} = 0.76$. This model reveals that the hydrodynamic size depends on the grafting density. In this study, the grafting density of PEG on AuNPs is

estimated by a thermogravimetric analysis (TGA) as reported.^{42,45} Fig. S3a–b shows the number of PEG (MW = 6000 Da) molecules per AuNP n and the grafting density $\sigma = n/(\pi D^2)$ for different particle sizes. The red line in Fig. S3a is a best fit to a polynomial function $n = a_2 D^2 + a_1 D + a_0$, where $a_2 = 0.762 \text{ nm}^{-2}$, $a_1 = 31.8 \text{ nm}^{-1}$ and $a_0 = 28$. The corresponding fit of σ is provided in Fig. S3b. Clearly, in our current size-range, the grafting density decreases with increased particle size. We note that grafting density can also be affected by the length of PEG. Nevertheless, for polymer ligands with fixed length, the trend of grafting density to decrease with decrease in surface curvature still holds. In fact, surface curvature plays an important role in the grafting density of thiolated molecules attached to gold. This behavior has been observed in experimental studies that aimed at determining the grafting density of PEG-SH (MW = 10000 Da) on AuNPs (similar in size to those reported here)⁴⁵ as well as in structural studies of short thiolated molecules grafted on smaller AuNPs.⁵⁰ Using the measured grafting density and the dynamic size of PEG-AuNPs and its trend versus Au core size are predicted by Eq. S1, as shown in Fig. S3c in good agreement with the measured values.

UV-Vis Spectra of AuNPs

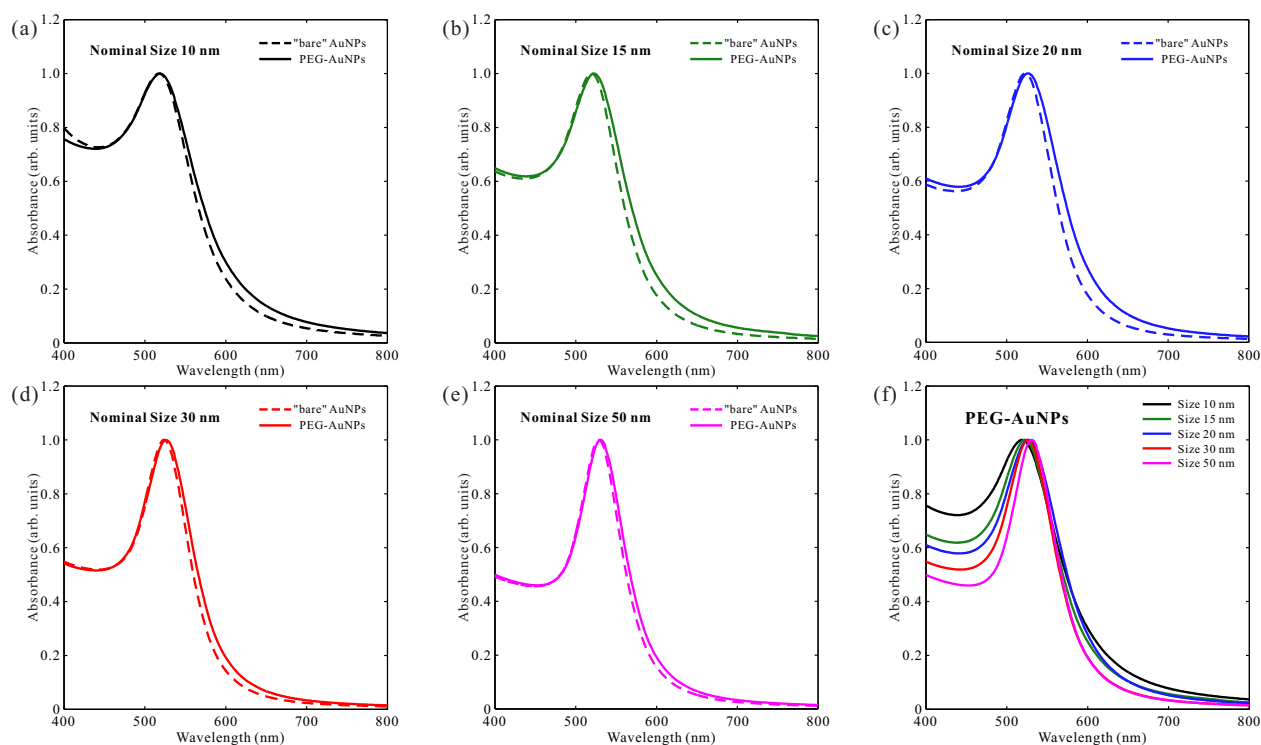


Fig. S4 UV-Vis spectra for unfunctionalized (bare) AuNPs and PEG-AuNPs with different nominal core sizes: (a) 10 nm, (b) 15 nm, (c) 20 nm, (d) 30 nm, (e) 50 nm. (f) Comparison of absorption for PEG-AuNPs with various nominal sizes.

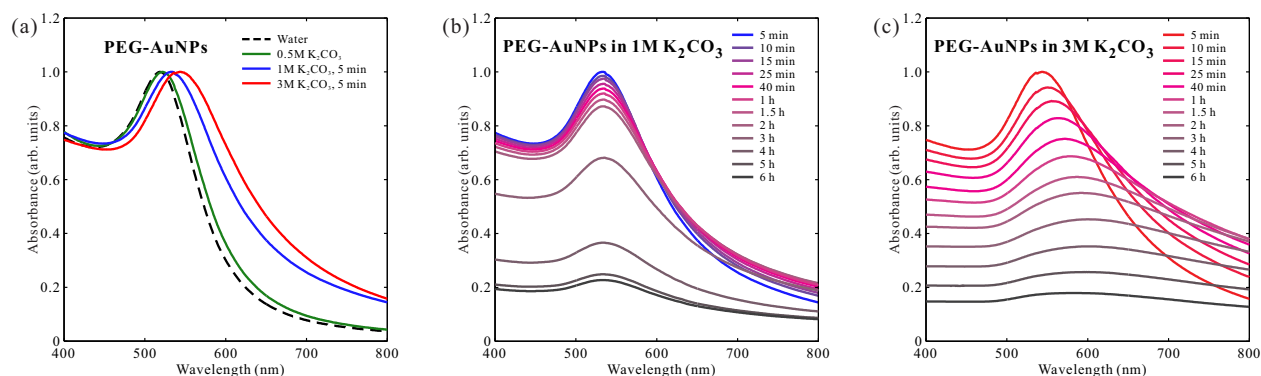


Fig. S5 UV-Vis spectra for PEG-AuNPs with Au core size of 10 nm in the presence of K_2CO_3 . (a) Absorption of PEG-AuNPs measured in water and 0.5–3M K_2CO_3 . The time dependence of adsorption takes place for PEG-AuNPs in the presence of (b) 1M K_2CO_3 and (c) 3M K_2CO_3 . Only the spectra for PEG-AuNPs in 1M and 3M K_2CO_3 measured at 5 min after sample preparation were plotted in (a) for comparison.

The UV-Vis absorption of unfunctionalized (bare) AuNPs stabilized with citrate and PEG-AuNPs in aqueous solution is measured by a UV-Visible spectrophotometer. Figure S4 shows spectra of AuNPs (with nominal core sizes 10–50 nm) in water before and after PEG

coating. The slight red shift (2–3 nm) of surface plasmon resonance (SPR) peaks corresponds to the ligand change on nanoparticle surfaces.

The absorption of PEG-AuNPs is changed when PEG-AuNPs are exposed to K_2CO_3 solutions. PEG-AuNPs are stable in water and low concentration K_2CO_3 solutions (≤ 0.5 M), while visible macroscopic precipitates are formed after hours at high concentration of K_2CO_3 (≥ 1 M). Figure S5a shows UV-Vis spectra for PEG-AuNPs with nominal core size of 10 nm in the absence and presence of K_2CO_3 . SPR peaks shift to longer wavelengths with the increase of K_2CO_3 concentrations, as adding K_2CO_3 increases the refractive index of the media where PEG-AuNPs are dispersed. No clear adsorption change is observed within months for PEG-AuNPs in water and in 0.5M K_2CO_3 . However, the spectra intensity decrease dramatically along with SPR peak broadening for PEG-AuNPs at higher concentration of K_2CO_3 as shown in Fig. S5b–c, which reveals nanoparticle aggregation takes place at high level of salts. Upon close inspection of the kinetics of the spectra on the same timescale, we note that the SPR peaks do not shift within hours at 1M K_2CO_3 , while there is a strong red-shift of SPR peaks measured at 3M K_2CO_3 , indicating that 1M and 3M K_2CO_3 affect the aggregation of PEG-AuNPs differently. In particular, at 3M K_2CO_3 , PEG-AuNPs are in close proximity to each other, thus SPR peaks shift to longer wavelength due to the plasmon coupling among nearest neighbor NPs.

Full Profile Analysis of SAXS

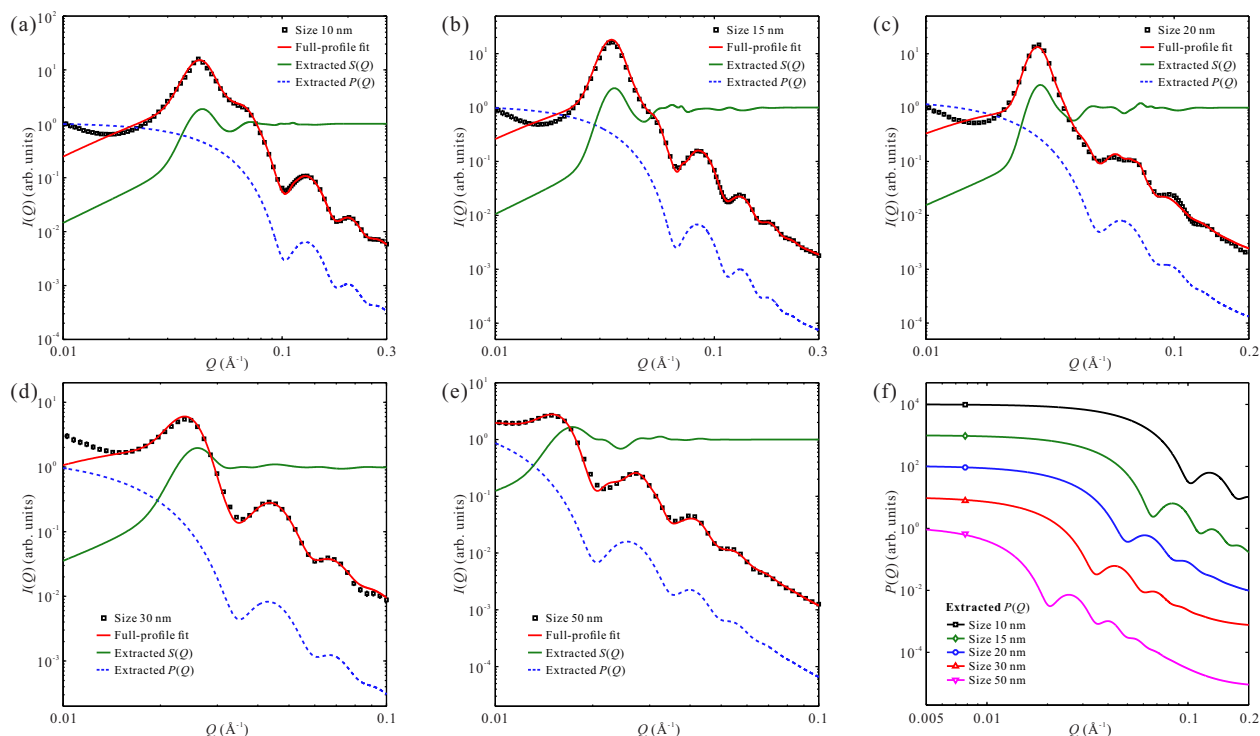


Fig. S6 Full profile analysis with extracted form factor $P(Q)$ and structure factor $S(Q) = I(Q) / [N_p P(Q)]$ for SAXS data of PEG-AuNP assemblies with different nominal core sizes: (a) 10 nm, (b) 15 nm, (c) 20 nm, (d) 30 nm, (e) 50 nm. (f) Comparison of the extracted $P(Q)$ from full profile fits. All the plots are vertically shifted for display purpose.

Full profile analysis of SAXS data from particle assemblies (including all peaks as well as form factor and potential diffuse scattering) provides higher accuracy and more information than solely analyzing a collection of decomposed peaks.⁴⁷ According to the literature,^{46–48} for a system of single-type components, when particle size polydispersity, diffuse scattering and local positional fluctuations are considered, the overall scattering intensity from ordered particle assemblies is given by

$$I(Q) = N_p P(Q) \{1 + [Z(Q) - 1] \beta(Q) G(Q)\}, \quad (S2)$$

where N_p is the number of particles, $P(Q) = \langle |F(\mathbf{Q})|^2 \rangle$ is the form factor with $F(\mathbf{Q})$ being the form factor amplitude, $\beta(Q) = \langle |F(\mathbf{Q})|^2 \rangle / P(Q)$ is the diffuse scattering, $G(Q) = \exp[-\sigma_D^2 Q_{hkl}^2 d_n^2]$ is the isotropic Debye–Waller factor (d_n is the nearest neighbor distance, σ_D describes local positional fluctuation), and $Z(Q)$ is the lattice structure factor. $Z(Q)$ is expressed as

$$Z(Q) = \sum_{hkl} Z_0(Q_{hkl}) \Pi(Q; Q_{hkl}, \sigma), \quad (S3)$$

where $\Pi(Q; Q_{hkl}, \sigma)$ is the peak shape function. In this study, we use a Gaussian function with the position of peak center Q_{hkl} , spread of the peak σ , and the integrated area 1. $Z_0(Q_{hkl})$ is the sum of the squares of the phase factors of the (hkl) reflection, normalized by

the number of particles in a unit cell, the solid angle of the reciprocal space at Q_{hkl} and the dimensional measure (i.e. length, area or volume) of the unit cell.⁴⁸ For a three-dimensionally randomly oriented FCC structure, $Z_0(Q_{hkl})$ is written as

$$Z_0(Q_{hkl}) = \frac{8\pi^2}{a^3 Q_{hkl}^2} m_{hkl}, \quad (\text{S4})$$

where a is the lattice constant, and m_{hkl} is the multiplicity of the (hkl) reflection.

Table S3 Comparison between core sizes of PEG-AuNPs determined from profile-fitting of SAXS data collected from the suspension and the assemblies

Nominal size (nm)	Size of Au in suspension (nm)	Size of Au in assemblies (nm)
10	8.7 ± 0.8	8.7 ± 0.8
15	13.3 ± 1.2	13.3 ± 1.1
20	17.7 ± 1.9	17.8 ± 1.9
30	25.6 ± 2.5	25.4 ± 2.5
50	43.5 ± 4.0	43.3 ± 3.8

Figure S6a–e show results of full profile fitting as well as extracted form factor $P(Q)$ and structure factor $S(Q) = I(Q) / [N_p P(Q)]$ from best fits. The extracted $P(Q)$ for various Au sizes is shown in Fig. S6f and the corresponding refined size information is provided in Table S3. Overall, the particle size extracted from the full profile fitting of the assemblies is consistent with the sizes modeled directly from SAXS of nanoparticle suspension.

Calculation of Radial Distribution Function

The inverse Fourier transform of the structure factor $S(Q)$ results in the radial distribution function or pair distribution function $g(r)$, which is expressed as^{47,51}

$$g(r) = 1 + \frac{1}{2\pi^2 n_p} \int_0^\infty [S(Q) - 1] Q^2 \frac{\sin(Qr)}{Qr} dQ, \quad (\text{S5})$$

where n_p is the particle number density in the assemblies.

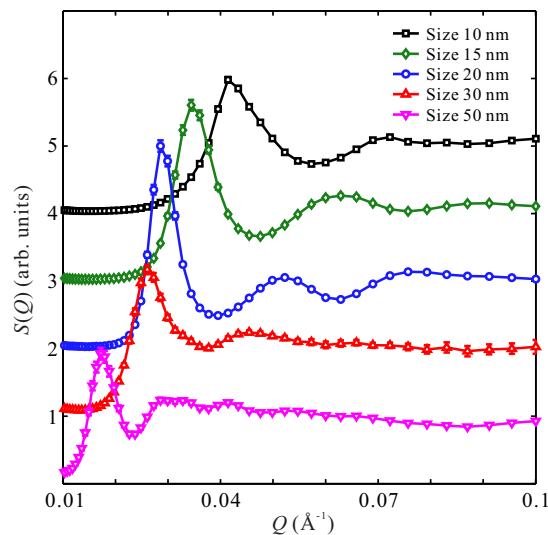


Fig. S7 The experimental structure factor $S(Q)$ for assemblies of PEG-AuNPs with different core sizes. Solid lines are guides to the eyes. All the plots are vertically shifted for display purpose.

The experimental structure factor $S(Q)$ is obtained by taking SAXS profiles from nanoparticle suspension as the experimental form factor $P(Q)$ and removing the experimental $P(Q)$ from the SAXS measurements of nanoparticle assemblies (Fig. S7). Here, $P(Q)$ is assumed to be the same for nanoparticles either distributed randomly in suspension or assembled into particle clusters, as $P(Q)$ and the corresponding particle size distribution extracted from full profile analysis of the assemblies are in good agreement with the experimental $P(Q)$ and the modeled size information (Table S3).

In the present study, n_p is practically unknown. To a good approximation, $n_p = \sqrt{2}/(D+2h)^3$ for a close-packed particle assembly with perfect contact of each particle with a core-shell structure (core diameter D and shell thickness h). Simply, we take core size of AuNPs as D , and estimate the brush height of PEG shell capped on AuNPs to be 5 nm based on previous results of full profile-fitting.

We note that according to Equation S5, n_p only determines the amplitude of $g(r)$, and does not affect peak positions that provide direct valuable information of the nearest-neighbor distance.

Theoretical Considerations

Calculation of PEG parameters:

The density of PEG melt can be calculated as

$$\rho = \frac{M_1 N_K}{N_A b A_p} = \frac{M_1 N_K}{N_A b^3 v^2}, \quad (\text{S6})$$

where N_K is the number of PEG monomers in a Kuhn length, M_1 the molecular weight of a PEG monomer, N_A is the Avogadro number, b is the Kuhn length and A_p is the minimal cross section area of PEG. A_p can also be written in dimensionless terms in relation to the Kuhn length $v^2 = A_p/b^2$ where $v < 1$. Agreement between Eq. S6 and the known density of PEG $\rho = 1.123 \text{ g/cm}^3$, implies using the same parameters as in our previous study,

$$v^2 = 0.341 \quad \text{or} \quad v = 0.584. \quad (\text{S7})$$

Polymer brush model:

In a recent publication by Zhang et al.⁴² it has been argued that the PEG shell in the functionalized PEG-AuNP is at the θ point and the boundary of the shell is under effective gradient surface-tension at the PEG/salt-solution interface. This is the result of osmotic pressure build-up by the difference in ion concentrations inside and outside the polymer shell, due the well known phase separation of PEG in salt solutions in general. It should be noted that the salt-rich environment that defines the outside of a PEG-AuNP in bulk is a poor solvent for PEG. Thus, decreasing the solvent quality by increasing salt concentration leads to a collapse transition where the PEG-AuNP becomes insoluble. It is at this point that the 3D supercrystals are formed by a process of colloidal destabilization.

The nearest neighbor distance d_n between PEG-AuNPs can be obtained by assuming that the formed precipitate (i.e., crystals) has negligible amounts of solvent, both ions and water. In this study, the PEG density in the 3D assemblies at 3M K_2CO_3 is estimated to be 0.77–1.43 g/cm^3 based on the measured nearest-neighbor distance of AuNPs and grafting density of PEG. Given the fact that the known density of PEG is 1.123 g/cm^3 , it is reasonable to assume that the amount of liquid (water and ions) is negligible. As discussed in the context of NPs capped with hydrocarbon ligands⁴⁹, it is convenient to consider the PEG-NP packing fraction (depends on symmetry), defined as

$$\eta_m = \frac{\text{Volume of material}}{\text{Total volume}} = \frac{4\pi R^3 + A_p L n}{V_{WS}(d_n)}, \quad (\text{S8})$$

where R is the core-radius of the AuNP, A_p is the cross section of a PEG polymer, L its maximum length, n the number of chains per NP and $V_{WS} \equiv V_{0,WS} d_n^3$ is the volume of the Wigner-Seitz cell (Note that $V_{0,WS}$ is a dimensionless volume that depends on the crystal symmetry and that we assume that A_p is the same for a monomer or a Kuhn length unit). Following standard conventions, we define the softness $\lambda = L/R$ and dimensionless coverage as $\xi = A_p \sigma \equiv A_p/A_0 < 1$. With this notation, Eq. S8 becomes

$$\eta_m = \frac{\pi}{6V_0} \left(\frac{2R\tau}{d_n} \right)^3 = \eta_{HS} \left(\frac{2R\tau}{d_n} \right)^3, \quad (\text{S9})$$

where $R\tau$ is the hydrodynamic radius of the PEG-NPs, η_{HS} is the hard sphere packing fraction for the corresponding lattice, in this case $\eta_{HS} = \frac{\pi}{3\sqrt{2}} \approx 0.7405$ for a closed packed fcc or hcp structure. The equation of state becomes

$$\mu = \left(1 + 3\sigma \frac{A_p L}{R} \right)^{1/3} = (1 + 3\xi\lambda)^{1/3} = \left(1 + 3 \frac{N b^3 \sigma v^2}{R} \right)^{1/3}, \quad (\text{S10})$$

where to obtain the last expression, Eq. S7 has been employed. There are two obvious choices for the nearest neighbor distance d_n , namely

$$\tau \equiv \frac{d_n}{2R} = \begin{cases} \frac{d_{OPM}}{2R} = \mu & (\eta_m = \eta_{HS}) \\ \frac{d_{MIN}}{2R} = \eta_{HS}^{1/3} \mu & (\eta_m = 1) \end{cases} \quad (\text{S11})$$

The first result is known as the optimal packing model (OPM)⁵² and is satisfied for high grafting densities $\xi \sim 1$ and short ligands $\lambda \lesssim 2$. The second is the minimum possible separation, where the polymer is distributed as a melt with maximal constant density. As discussed in Ref⁴⁹, separations $d_n < d_{OPM}$ involve polymer textures that require consideration of topological defects.